Research Article

Identification of predictive MRI and functional biomarkers in a pediatric piglet traumatic brain injury model

https://doi.org/10.4103/1673-5374.290915

Received: October 10, 2019

Peer review started: October 17, 2019

Accepted: January 10, 2020

Published online: August 24, 2020

Hongzhi Wang[1], Emily W. Baker[2, 3], Abhyuday Mandal[1], Ramana M. Pidaparti[4], Franklin D. West[2, 3, *], Holly A. Kinder[2, 3, *]

Abstract

Traumatic brain injury (TBI) at a young age can lead to the development of long-term functional impairments. Severity of injury is well demonstrated to have a strong influence on the extent of functional impairments; however, identification of specific magnetic resonance imaging (MRI) biomarkers that are most reflective of injury severity and functional prognosis remain elusive. Therefore, the objective of this study was to utilize advanced statistical approaches to identify clinically relevant MRI biomarkers and predict functional outcomes using MRI metrics in a translational large animal piglet TBI model. TBI was induced via controlled cortical impact and multiparametric MRI was performed at 24 hours and 12 weeks post-TBI using T1-weighted, T2-weighted, T2-weighted fluid attenuated inversion recovery, diffusion-weighted imaging, and diffusion tensor imaging. Changes in spatiotemporal gait parameters were also assessed using an automated gait mat at 24 hours and 12 weeks post-TBI. Principal component analysis was performed to determine the MRI metrics and spatiotemporal gait parameters that explain the largest sources of variation within the datasets. We found that linear combinations of lesion size and midline shift acquired using T2-weighted imaging explained most of the variability of the data at both 24 hours and 12 weeks post-TBI. In addition, linear combinations of velocity, cadence, and stride length were found to explain most of the gait data variability at 24 hours and 12 weeks post-TBI. Linear regression analysis was performed to determine if MRI metrics are predictive of changes in gait. We found that both lesion size and midline shift are significantly correlated with decreases in stride and step length. These results from this study provide an important first step at identifying relevant MRI and functional biomarkers that are predictive of functional outcomes in a clinically relevant piglet TBI model. This study was approved by the University of Georgia Institutional Animal Care and Use Committee (AUP: A2015 11-001) on December 22, 2015.

Key Words: controlled cortical impact; gait analysis; linear regression; magnetic resonance imaging; motor function; pediatric pig model; principal component analysis; traumatic brain injury

Chinese Library Classification No. R445; R364; R741

Introduction

In United States, traumatic brain injury (TBI) is a leading cause of long-term and permanent disability and even death. Each year, approximately 2.8 million people suffer from a TBI in the United States (Taylor et al., 2017). Unfortunately, one of the largest groups affected by TBI are children between the age of 0 and 14 with almost half a million (473,947) children going to the ER each year (Faul et al., 2010). After TBI in these patients, one of the major questions has become how to reliably predict functional outcomes and recovery with significant efforts being made in the use of non-invasive imaging modalities including magnetic resonance imaging (MRI) (Galloway et al., 2008; Guild and Levine, 2015).

MRI is widely used in TBI patients and has significant potential to identify key changes in pathophysiology that can be utilized to predict functional outcomes in patients (Saatman et al., 2008; Cooper et al., 2014). MRI is capable of assessing TBI progression longitudinally and providing comprehensive information on spatiotemporal parameters such as lesion volume and midline shift (Chastain et al., 2009; Lee et al., 2012). In humans, TBI tissue damage detected by MRI was found to be related with gait and balance deficits (Caeyenberghs et al., 2010; Drijkoningen et al., 2017). In pediatric TBI patients, regional gray matter volume was positively correlated with gait control as indicated by loss of gray matter volume coinciding with increased step length asymmetry (Drijkoningen et al., 2017). This suggests that these MRI "biomarkers" might be a powerful tool to predict injury recovery.

Rodent models are widely used to study TBI pathophysiology,

[1]Department of Statistics, University of Georgia, Athens, GA, USA; [2]Regenerative Bioscience Center, University of Georgia, Athens, GA, USA; [3]Department of Animal and Dairy Science, University of Georgia, Athens, GA, USA; [4]College of Engineering, University of Georgia, Athens, GA, USA
*Correspondence to: Holly A. Kinder, PhD, HollyK17@uga.edu; Franklin D. West, PhD, westf@uga.edu.
https://orcid.org/0000-0001-8310-7265 (Holly A. Kinder); https://orcid.org/0000-0002-0504-7997 (Franklin D. West)

Funding: *Financial support was provided by the University of Georgia Office of the Vice President for Research to FDW.*
How to cite this article: *Wang H, Baker EW, Mandal A, Pidaparti RM, West FD, Kinder HA (2021) Identification of predictive MRI and functional biomarkers in a pediatric piglet traumatic brain injury model. Neural Regen Res 16(2):338-344.*

motor function deficits and to perform safety and efficacy studies for potential treatments (Marklund, 2016). However, failure to develop a Food and Drug Administration (FDA) approved treatment despite numerous clinical trials, with more promising therapeutics failing to reach primary end points in phase III trials, has led to increased interest in more translational and predictive animal models (Jain, 2008). The pig has become a TBI model of significant interest due to increased similarities to humans in terms of brain anatomy, physiology and development (Dobbing and Sands, 1979; Flynn, 1984; Gieling et al., 2011; Conrad et al., 2012; Costine et al., 2015; Paredes et al., 2016). Also, given that children are more likely to sustain a concussive TBI after a fall, the use of a juvenile model that more closely recapitulates this type of injury, such a piglet controlled cortical impact (CCI) model, is critical for the study of TBI outcomes and the development of potential therapeutics that are specific for a pediatric population (Baker et al., 2019). Compared to the rodent brain, the piglet brain has been found to more closely mirror the pediatric human brain in terms of brain size, time scale of myelination, and total white matter volume, which are important factors to consider when a TBI occurs during development when the brain is most vulnerable to injury (Kinder et al., 2019a).

To date, there are only a limited number of studies that assess TBI pathophysiology utilizing MRI in pig models. T1- and T2-weighted sequences are the most commonly used MRI sequences to measure lesion volumes in the TBI pig model (Duhaime et al., 2003; Grate et al., 2003; Rosenthal et al., 2008; Karlsson et al., 2018) and diffusion tensor imaging (DTI) and diffusion-weighted imaging (DWI) have been used to measure white matter integrity and brain microstructure (Conrad and Johnson, 2015). However, there are no pig studies that have taken a quantitative statistical approach to assessing the longitudinal relationship between MRI observed TBI pathology (e.g., lesion volume) and motor function changes in a pediatric pig model. Given the heterogeneity of TBI, there remains a lack of biomarkers of TBI outcome that have consistent prognostic value across the human TBI population. Therefore, a major goal of this study is to identify TBI outcome biomarkers with high predictive value and clinical relevance using a more translational pig TBI model.

The objective of this study was to utilize advanced statistical approaches to identify key MRI parameters that are longitudinally associated with changes in motor function in a piglet TBI model. In this study, we utilized principal component analysis (PCA) on six MRI parameters and 12 gait parameters collected in a CCI TBI piglet model to identify parameters that explain the most variability of the data. Furthermore, this information was used to determine if MRI biomarkers can be used to predict motor function impairments via linear regression analysis. This study provides an important first step in understanding the predictive power of MRI biomarkers and motor function outcomes in a pediatric TBI model that more closely resembles human TBI patients than traditional rodent models.

Materials and Methods

Animals and CCI surgery

Data that underwent advanced statistical analysis was collected as part of a previously published study (Kinder et al., 2019b). Briefly, all work was performed in accordance with the University of Georgia Institutional Animal Care and Use Committee guidelines (AUP: A2015 11-001, approved on December 22, 2015). Eighteen commercially bred, male piglets were born at the Large Animal Research Unit at the University of Georgia. All piglets were castrated for this study. It is not expected that pre-pubescent castrated or uncastrated males will have differing levels of sex hormones that would affect injury responses following TBI.

Piglets between 4–5 weeks of age underwent TBI induction surgery. On the day of surgery, piglets were anesthetized using 5% isoflurane and oxygen via surgical mask and then maintained under anesthesia during surgical procedures using 2.5–3% isoflurane. Vitals (temperature, heart rate, and respiration rate) were monitored every 5–10 minutes during anesthesia. Piglets were administered Flunixin (2.2 mg/kg) and butorphanol (0.2 mg/kg) as a pre-med for analgesia. The surgery site was prepared routinely for surgery. The surgical site was clipped, sterilized using Betadine and 70% ethanol, and covered with a sterile drape. A 4 cm left-sided incision was made over the top of the cranium to expose the underlying skull. A craniectomy, approximately 20 mm in diameter, was performed using an air driller (Brassler, Savannah, GA, USA) at the left anterior junction of the coronal and sagittal sutures to expose the underlying dura.

The piglet was moved onto a controlled cortical impact (CCI) device (University of Georgia Instrument Design and Fabrication Shop; Athens, GA, USA) as previously described (Baker et al., 2019; Kinder et al., 2019b). A 15 mm impactor tip was positioned over the intact dura to induce injury with the following parameters: 4 m/s velocity, 9 mm depth of depression, and 400 ms dwell time. Immediately following CCI, the surgical site was flushed with sterile saline and re-apposed with surgical suture without replanting the bone flap. After surgery, piglets were maintained on oxygen until recovered and then placed back in their home pens once ambulatory. For post-operative analgesia, piglets were administered Flunixin (2.2 mg/kg) 12 hours post-surgery and then once daily for an additional 4 days. Oxytetracycline (19.8 mg/kg) was administered as an antibiotic for 5 days post TBI. Piglets were monitored daily for health or signs of abnormal neurological behaviors.

To assess changes over time after TBI, piglets were separated into four groups based on sacrifice date: 24 hours (n = 4), 1 week (n = 4), 4 weeks (n = 4), and 12 weeks (n = 6) post-TBI (**Additional Figure 1**).

Magnetic resonance imaging

Magnetic resonance imaging (MRI) was performed 24 hours and 12 weeks post-TBI on a clinical 3.0 Tesla whole-body MR scanner (Siemens MAGNETOM TIM/Trio system, Siemens Healthineers, Erlangen, Germany) using a 12-channel phased array head coil. During MRI acquisition, pigs were maintained under anesthesia using the protocol described for CCI induction and positioned in dorsal recumbency. Standard multiplanar MR brain imaging sequences were performed at the sagittal, coronal, and axial planes including T2-weighted (T2W) fast spin echo (FSE), T2-weighted fluid attenuated inversion recovery (FLAIR), axial DWI, and DTI. Due to acquisition complications, group sizes were as follows: T2-weighted FSE and FLAIR, n = 5 at 24 hours and 12 weeks post-TBI; DWI and DTI, n = 6 at 24 hours post-TBI and n = 5 at 12 weeks post-TBI (**Additional Figure 1**).

T2W images were used for volumetric assessments such as lesion volume, which was defined by pixels with abnormal (high or low) signal intensity compared to the same anatomic area on the contralateral hemisphere. To calculate lesion volume, OsiriX DICOM Viewer (Bernex, Switzerland) was used to manually define the lesion on a slice by slice basis. The area of each slice was multiplied by the slice thickness (5 mm) to obtain the lesion volume of each slice. The slice areas were then summed to obtain total lesion volume. T2W images were also used to measure midline shift which is defined as the maximal horizontal displacement of the septum pellucidum in relation to the midline (Jacobs et al., 2011; Sauvigny et al., 2016). The distance from the septum pellucidum to the outer border of the cortex was measured for each hemisphere. The midline shift was calculated using the formula: midline shift (mm) = (total diameter/2) – contralateral diameter.

DWI sequences were used to generate apparent diffusion coefficient (ADC) maps to measure changes in diffusivity. Mean ADC values were calculated with NIH ImageJ software at a manually drawn region of interest (ROI) that was defined by pixels with abnormal (high or low) signal intensity compared to the same anatomic area on the contralateral hemisphere. The ROI did not delineate between the lesion core and perilesion tissue. All hypointense and hyperintense regions were included in the ROI as lesion tissue. A ROI drawn in a symmetrical site in the contralateral hemisphere served as an internal control. Mean ADC values were obtained by calculating the average signal intensity across all slices. Normalized ADC value was calculated by dividing the ipsilateral ADC value by the contralateral ADC value. All ADC values are reported as 10^{-3} mm^2/s.

DTI sequences were used to generate fractional anisotropy (FA) maps to measure changes in white matter integrity. ROIs were drawn at the internal capsule (IC) and corpus callosum (CC) on one representative slice per animal using NIH ImageJ software at the ipsilateral and contralateral side of the injury (Schindelin et al., 2015). Normalized FA value was calculated by dividing the ipsilateral FA value by the contralateral FA value for both the IC and CC.

Gait analysis

Pigs underwent gait assessment at the following time points: 24 hours (n = 18) and 12 weeks post-TBI (n = 6). Gait was collected using a GAITFour® electronic, pressure-sensitive mat (CIR Systems Inc., Franklin, NJ, USA) that is 7.01 m in length and 0.85 m in width with an active area that is 6.10 m in length and 0.61 m in width. In this arrangement, the active area is a grid, 48 sensors wide by 480 sensors long, totaling 23,040 sensors. Prior to gait collection, pigs were trained to travel back and forth across the gait mat at a self-selected, consistent two-beat gait using food as a positive reward. During gait collection, pigs were assessed until 4–5 consistent trials were obtained, or up to a maximum of 20 minutes per pig on each testing day. For each trial, a minimum of three gait cycles with less than 10% variability in velocity were selected, and all gait parameters were calculated automatically using the GAITFour® software. Age-matched, male normal pigs (n = 6) were born at the Large Animal Research Unit at the University of Georgia and underwent gait collection at identical time points to TBI pigs in order to account for changes in gait that are attributed to normal growth. The gait parameters assessed are described in **Table 1**. The following parameters are reported as an average in step length, stride length, percent swing, percent stance, number of sensors, scaled pressures, mean pressure, hind reach, total pressure index, and step/stride ratio in left front, right front, left hind, and right hind limbs.

Table 1 | **Gait parameter definitions**

Gait parameter	Definition
Spatial parameters	
Step length	Distance between corresponding successive points of heel contact of opposing limbs (i.e., right front and left front, right hind and left hind); expressed in cm
Stride length	Distance between successive points of heel contact of the same hoof (i.e., left front and left front); expressed in cm
Hind reach	Distance from the heel center of the hind limb to the heel center of the previous front limb on the same side (i.e., left hind to left front); expressed in cm
Step/stride ratio	The ratio between step and stride lengths of the same limb
Number of sensors	The number of sensors activated by contact of each limb
Temporal parameters	
Velocity	Stride Length divided by stride time, expressed in cm/s
Cadence	Frequency of steps/min during a trial
Percent stance	Percentage of time during which a limb is in stance phase during one stride cycle (stance time/cycle time)
Percent swing	Percentage of time during which a limb is in swing phase during one stride cycle (swing time/cycle time)
Pressure parameters	
Mean pressure	Average pressure of all sensors for one limb
Total scaled pressure	The sum of peak pressure values recorded from each activated sensor by a limb during mat contact, represented by the switching levels and reported as a scaled pressure from 0–7 for each sensor
Total pressure index (TPI)	Percent distribution of weight across all four limbs. Pigs typically carry 30% of their weight in each front limb and 20% of their weight in each hind limb

Statistical analysis

PCA is an unsupervised dimension reduction technique that generates linear combinations of the original variables by exploring sources of variation within the data set. The first principal component explains the greatest sources of variation and the subsequent PCs explain the greatest sources of variation beyond the first PC. In PCA, the first assumption is that the data cannot have missing values. The second assumption is that the sample size (denoted as n) of data should be greater than or equal to the number of parameters (denoted as p). The third assumption is that parameters of data should be at least moderately correlated with each other.

PCA was performed using five MRI parameters, normalized ADC, normalized IC FA, normalized CC FA, lesion volume, and midline shift. PCs for the MRI data are linear combinations of those five parameters, written as $PC_i = a_{i1}$ ADC + a_{i2} ICFA + a_{i3} CCFA + a_{i4} lesion volume + a_{i5} midline shift, where i = 1, 2, …, 5. When some of the a_i's are equal to zero, PCs are linear combinations of one or more parameters out of five parameters, and each PC corresponds to a unique linear combination. PCA was implemented separately at 24 hours and 12 weeks post-TBI.

PCA was also performed using twelve gait parameters listed and described in **Table 1**. Similarly, PCs for the gait data are linear combinations of those twelve parameters, written as $PC_i = a_{i1}$ Step Length + a_{i2} Stride Length + a_{i3} Hind Reach + … + $a_{i,12}$ TPI, where i = 1, 2, …, 12. When some of the a_i's are equal to zero, PCs are linear combinations of several parameters out of twelve parameters, and each PC corresponds to a unique linear combination. PCA was implemented separately at 24 hours and 12 weeks post-TBI. Biplots were generated to illustrate a coordinate system for PCs for both MRI and gait data. Simple linear regression was utilized to determine whether MRI parameters are able to predict gait parameters with respect to functional changes. P-values ≤ 0.05 were considered to be statistically significant. All statistical analysis was performed using R (R Core Team, 2013).

Results

Lesion volume and midline shift explain most of the MRI data variability at 24 hours and 12 weeks post-TBI

Representative T2W images 24 hours (**Figure 1A**) and 12 weeks (**Figure 1B**) post-TBI images show distinct brain lesions. At 24 hours post-TBI, the midline shifted away from the ipsilateral hemisphere (**Figure 1C**, red line) at the level of the septum pellucidum (yellow line), while at 12 weeks post-TBI the midline shifted toward the ipsilateral hemisphere (**Figure 1D**, blue line). These changes in midline shift are indicative of swelling and atrophy at each time point, respectively. At 24 hours and 12 weeks post-TBI, PCA analysis of lesion volume and midline shift from T2W sequences, normalized ADC from DWI sequences, and normalized IC and CC FA values from DTI sequences was performed. The scree plot of the five PCs of MRI data at 24 hours post-TBI using covariance criteria showed that PC1 and PC2 explained most of the variability

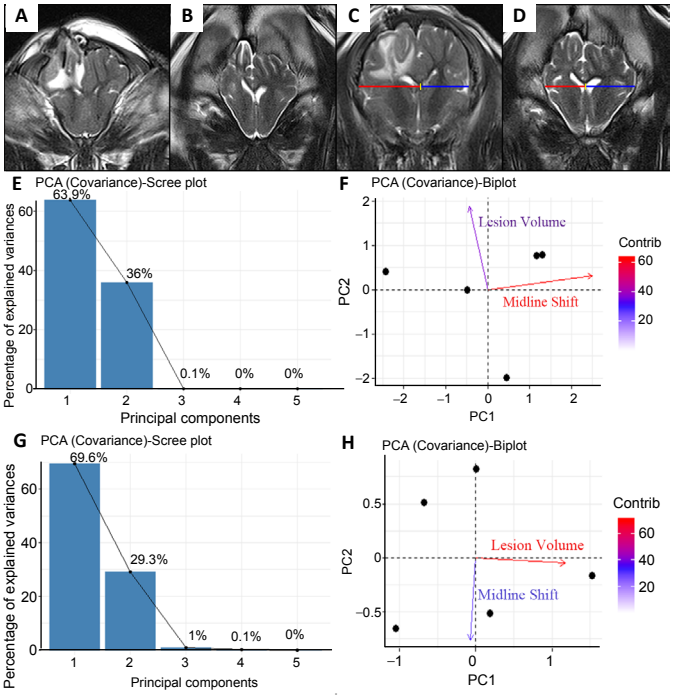

Figure 1 | **Lesion volume and midline shift explain most of the MRI data variability at 24 hours and 12 weeks post-TBI.**
Representative T2-weighted Fast Spin Echo images 24 hours (A) and 12 weeks (B) post-TBI images show distinct brain lesions. At 24 hours post-TBI, the midline shifted away from the ipsilateral hemisphere (C, red line) at the level of the septum pellucidum (C, yellow line), while at 12 weeks post-TBI the midline shifted toward the ipsilateral hemisphere (D, blue line). The scree plot of the five PCs at 24 hours post-TBI using covariance criteria showed that PC1 and PC2 explained most of the variability (E). The biplot of PC1 against PC2 of indicated that lesion volume and midline shift is dominant in explaining most of the variability at 24 hours post-TBI (F). The scree plot of the five PCs at 12 weeks post-TBI using covariance criteria showed that PC1 and PC2 explained most of the variability (G). The biplot of PC1 against PC2 indicated that lesion volume and midline shift is dominant in explaining most of the variability at 12 weeks post-TBI (H). MRI: Magnetic resonance imaging; PC: principal component; TBI: traumatic brain injury.

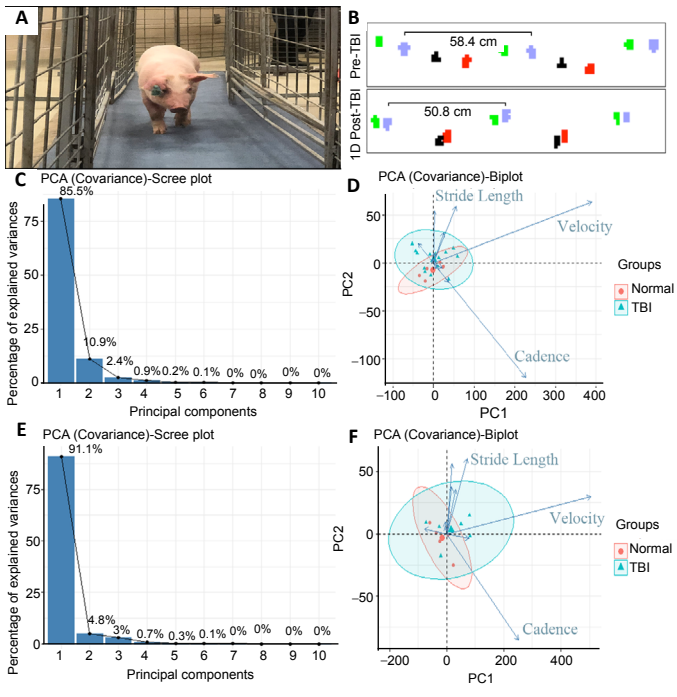

Figure 2 | **Velocity, cadence, and stride length explain most of the gait data variability at 24 hours and 12 weeks post-TBI.**
Pigs were subjected to gait analysis using a GAITFour® electronic, pressure-sensitive mat at 24 hours and 12 weeks post-TBI (A). Activated sensors on the mat were capable of detecting key gait pressure and spatiotemporal parameter changes of the left front (blue), left hind (green), right front (red), and right hind (black) limbs (B). The scree plot of the first 10 PCs of gait data at 24 hours post-TBI using covariance criteria showed that PC1 and PC2 explained most of the variability (C). The biplot of PC1 against PC2 indicated that velocity, cadence, and stride length are dominant in explaining most of the variability at 24 hours post-TBI (D). The scree plot of the first 10 PCs of gait data at 12 weeks post-TBI using covariance criteria showed that PC1 and PC2 explained most of the variability (E). The biplot of PC1 against PC2 indicated that velocity, cadence, and stride length are dominant in explaining most of the variability at 12 weeks post-TBI (F). PC: Principal component; PCA: principal component analysis; TBI: Traumatic brain injury.

(63.9% and 36%, respectively, **Figure 1E**). Both PC1 and PC2 are linear combinations of lesion volume and midline shift (**Figure 1E**). The biplot of PC1 against PC2 indicated that lesion volume and midline shift are dominant in explaining most of the variability at 24 hours post-TBI (**Figure 1F**). The scree plot of the five PCs of MRI data at 12 weeks post-TBI using covariance criteria showed that PC1 and PC2 explained most of the variability (69.6% and 29.3%, respectively, **Figure 1G**). Both PC1 and PC2 are linear combinations of lesion volume and midline shift (**Figure 1G**). The biplot of PC1 against PC2 indicated that lesion volume and midline shift are dominant in explaining most of the variability at 12 weeks post-TBI (**Figure 1H**). Taken together, these results suggest that lesion volume and midline shift are key MRI indicators of injury severity after TBI.

Velocity, cadence, and stride length explain most of the gait data variability at 24 hours and 12 weeks post-TBI

Pigs were subjected to gait analysis using a GAITFour® electronic, pressure-sensitive mat at 24 hours and 12 weeks post-TBI (**Figure 2A**). Activated sensors on the mat were capable of detecting key gait pressure and spatiotemporal parameter changes of the left front (blue), left hind (green), right front (red), and right hind (black) limbs (**Figure 2B**, black line indicates stride length for the left front limb). The scree plot of the first 10 PCs of gait data at 24 hours post-TBI using covariance criteria showed that PC1 and PC2 explained most of the variability (85.5% and 10.9%, respectively, **Figure 2C**). Only the first 10 PCs are displayed because the percentage of explained variances of the last 6 PCs (PC7-PC12) are all 0%. PC1 is a linear combination of velocity, cadence, and stride length, while PC2 is a linear combination of velocity, cadence, step length, stride length, percent swing, percent stance, and total scaled pressure (**Figure 2C**). The biplot of PC1 against PC2 indicated that velocity, cadence, and stride length are dominant in explaining most of the variability at 24 hours post-TBI (**Figure 2D**). The Scree Plot of the first 10 PCs of gait data at 12 weeks post-TBI using covariance criteria showed that PC1 and PC2 explained most of the variability (91.1% and 4.8%, respectively, **Figure 2E**). Similarly, only the first 10 PCs are displayed because the percentage of explained variances of the last 6 PCs (PC7-PC12) are all 0%. PC1 is a linear combination of velocity, cadence, stride length, percent swing, and percent stance, while PC2 is a linear combination of velocity, cadence, step length, stride length, total scaled pressure, and hind reach (**Figure 2E**). The biplot of PC1 against PC2 indicated that velocity, cadence, and stride length are dominant in explaining most of the variability at 12 weeks post-TBI (**Figure 2F**). Taken together, these results suggest that velocity, cadence, and stride length are key gait indicators of motor function impairments after TBI.

Lesion volume and midline shift predict deficits in stride and step length

Linear regression analysis was performed to determine if MRI parameters predict changes in gait. Combined 24-hour and 12-week post-TBI data showed that increases in lesion volume resulted in a direct decrease in stride length (**Figure**

3A) and step length (**Figure 3B**). Lesion volume was found to be significant in predicting stride length (P = 0.03) and step length (P = 0.02; **Table 2**). Similarly, an increase in midline shift resulted in a direct decrease in stride length (**Figure 3C**) and step length (**Figure 3D**). Midline shift was found to be significant in predicting stride length (P = 0.03) and step length (P = 0.03; **Table 2**). Therefore, these results suggest that lesion size and midline shift can be used as key indications of functional deficits in a pig TBI model.

Discussion

Multiparametric neuroimaging is becoming increasingly more important for identifying and diagnosing TBI outcomes (Sigmund et al., 2007; Chastain et al., 2009). However, the identification of key MRI biomarkers with potent prognostic value has proven to be challenging given the heterogeneous nature of TBI and the diversity of the patient population. Multivariate projection models may provide a mathematical framework to identify linear combinations of MRI biomarkers with acceptable sensitivity and specificity with regard to predicting outcome (Irimia et al., 2012). In this study, we performed PCA in order to explore the largest sources of variation within MRI datasets and identify MRI parameters that closely covary. We found that linear combinations of lesion size and midline shift explain most of the variability of the data at both 24 hours and 12 weeks post-TBI. In addition, PCA was utilized to explore the largest sources of variation within gait datasets and identify gait parameters that closely covary. Linear combinations of velocity, cadence, and stride length were found to explain most of the gait data variability at 24 hours and 12 weeks post-TBI. Linear regression of MRI and gait parameters combined at 24 hours and 12 weeks post-TBI revealed both lesion size and midline shift were negatively correlated with stride length and step length. Taken together, in this study we showed that advanced statistical approaches can be used to identify key, clinically relevant MRI biomarkers and predict functional outcomes using MRI metrics in a large animal piglet TBI model that closely recapitulates human TBI.

Injury responses following TBI are complex and heterogeneous which creates a challenging landscape for the development of effective diagnostic and prognostic tools (Ziebell and Morganti-Kossmann, 2010; Allen, 2016). Therefore, the identification and use of potent TBI biomarkers may aid in early diagnosis, guide treatment selections, and provide critical insight of long-term prognosis (Martinez and Stabenfeldt, 2019). The use of machine learning and multivariate statistical models may be well suited to identify potential TBI biomarkers by analyzing large data sets to reveal prospective markers of interest (Irimia et al., 2012; Mateos-Perez et al., 2018). In this study, we found that both PC1 and PC2 are linear combinations of lesion volume and midline shift at 24 hours and 12 weeks post-TBI which suggests that lesion volume and midline shift are key contributors to injury severity at both acute and chronic timepoints in this model. MRI assessments of lesion volume using conventional approaches such as T2W and FLAIR have been found to correspond to injury severity in both pre-clinical models and human TBI patients (Sigmund et al., 2007; Immonen et al., 2009). Increased lesion volume has been associated with poorer Glasgow Outcome Scale (GOS) scores in adult TBI patients and GOS-Extended Pediatrics (GOS-E Peds) scores in pediatric TBI patients (Chastain et al., 2009; Smitherman et al., 2016). Similarly, increased degree of midline shift in patients with head injuries by CT scan corresponded to injury severity, and a midline shift > 5 mm was predictive of reduced favorable outcomes and lower quality of life (Chiewvit et al., 2010; Swanson et al., 2012; Puffer et al., 2018). However, predictions of functional outcomes may be enhanced by using multivariate statistical classification methods that identify linear combinations of MRI metrics. The results from this study provide an important first step in identifying relevant MRI biomarkers of injury severity in a piglet model of TBI that can be used in future studies to predict a broad range of functional outcomes such as neurologic function, behavior, cognition and motor function.

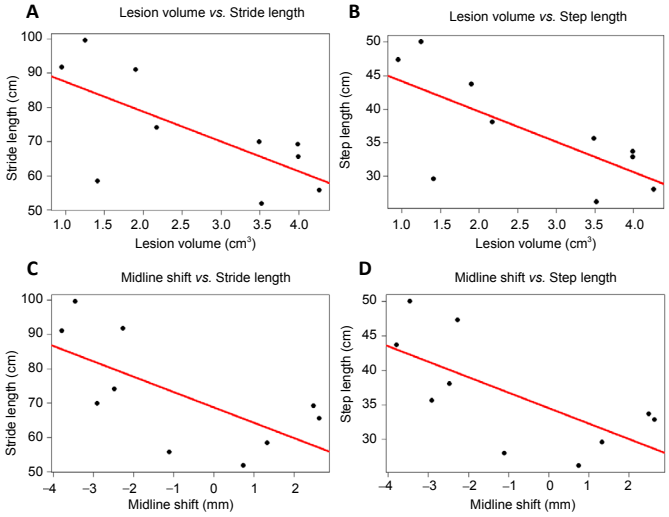

Figure 3 | Lesion volume and midline shift predict deficits in stride and step length.
Linear regression demonstrated that increases in lesion volume resulted in a direct decrease in stride length (A) and step length (B; $P < 0.05$). Increases in midline shift resulted in a direct decrease in stride length (C) and step length (D; $P < 0.05$).

Table 2 | Linear regression demonstrates that lesion volume predicts stride length and step length. Midline shift also predicts stride length and step length

Model of parameters	*P*-value
Stride length = 96.14 – 8.7 × lesion volume	0.0306
Step length = 48.68 – 4.52 × lesion volume	0.0219
Stride length = 68.79 – 4.45 × midline shift	0.0341
Step length = 34.5 – 2.26 × midline shift	0.0305

P-value of < 0.05 indicates significance.

Neural damage following TBI can lead to the development of balance instability, decreased motor control, and gait abnormalities (Caeyenberghs et al., 2009; Katz-Leurer et al., 2009a, b). These impairments can lead to changes in a multitude of spatiotemporal gait parameters such as velocity, cadence, step length, stride length, stance percent, and swing percent (Williams et al., 2009, 2010). Currently, it is not well studied if a single parameter, or combination of parameters, might be more sensitive to injury and thus more reflective of TBI outcomes. In this study, we found that velocity, cadence, and stride length were dominant in explaining most of the variability at 24 hours and 12 weeks post-TBI. A number of clinical studies have observed significant reductions in velocity and cadence following TBI that can persist for months to even years in both adult and pediatric populations (Kuhtz-Buschbeck et al., 2003; Beretta et al., 2009; Williams et al., 2009; Martini et al., 2011). Consequently, as a result of a decreased velocity and motor stability, stride length may also become reduced in TBI patients (Kuhtz-Buschbeck et al., 2003; Chou et al., 2004). To our knowledge, this is the first study in a piglet TBI model to provide important information regarding potential gait biomarkers for injury using PCA. These results can be used in future studies to better predict TBI outcomes.

TBI severity has been implicated to play an important role in motor function outcomes, especially in children who sustain a TBI at a young age (Gagnon et al., 2004). Increasing lesion size is well established to reflect TBI severity (Washington et al., 2012; Baker et al., 2019). In this study, simple linear regression

was performed to examine the relationship between lesion size and different spatiotemporal gait parameters. We found that increasing lesion size is predictive of decreases in stride and step length in this model. Similarly, increasing injury severity and lesion size have been found to be associated with motor function impairments in other pre-clinical rodent (Beaumont et al., 1999; Tsenter et al., 2008) and pig (Baker et al., 2019) TBI models. In pediatric TBI patients, increases in TBI severity were found to have a negative impact on motor performance and clinical measures (Jaffe et al., 1993; Kuhtz-Buschbeck et al., 2003). In addition, linear regression analysis in this study revealed that increases in midline shift are also predictive of decreases in step and stride length in this model. In human TBI patients, the presence of a midline shift > 5 mm was found to be associated with greater need of assistance with ambulation and worse GOS-E outcomes, but no direct comparisons to spatiotemporal gait parameters have been investigated (Englander et al., 2003; Puffer et al., 2018). The results from this study have identified an exciting and clinically translatable predictive relationship between the MRI parameters lesion size and midline shift and the gait spatiotemporal parameters stride length and step length. This use of this approach may aid in more precise predictions of motor impairments following TBI.

While this study shows the potential of PCA in identifying possible MRI biomarkers, there are a few limitations to our findings. First, the study sample size is limited and the analysis focused on only two timepoints after injury. The identification of prognostic measures using multivariate statistical models are more robust in TBI samples with larger sample sizes that enable the generation of more refined principal components. In addition, a longitudinal study with more intermediate and later gait and MRI time points would enable better characterization of dynamic changes and improved identification of potential TBI biomarkers. In this study, given the small sample size, data from 24 hours and 12 weeks post-TBI were combined to assess the relationship between MRI and gait outcomes. This prevented the use of acute MRI data to predict long-term functional outcomes. In the future, a study with a larger sample size will allow for enhanced identification of MRI biomarkers at early timepoints that predict unfavorable motor function outcomes long-term. Furthermore, inherent differences in brain cytoarchitecture and vasculature between individuals are a major factor of the heterogeneous responses following TBI (i.e., differences in brain collateralization). In future studies with larger cohorts, predicting functional outcomes may be more accurate by grouping animals with unique injury types, such as hemorrhage volume or necrosis volume.

Conclusions

In this study we have utilized advanced statistical approaches to identify potential MRI and functional biomarkers in a piglet TBI model. Principal component analysis revealed that the MRI parameters lesion volume and midline shift and the gait parameters velocity, cadence, and stride length may serve as potential biomarkers that are most reflective of TBI outcomes. Lesion volume and midline shift were also found to be significantly correlated with changes in stride and step length which lends support to the clinical utilization of MRI biomarkers to predict motor function outcomes. In the future, this model can be used to further explore the prognostic value of MRI biomarkers in predicting other functional outcomes such as behavior and cognition.

Acknowledgments: *We would like to thank Richard Utley and Kelly Parham for their animal assistance; Vivian Lau and Lisa Reno for their surgical expertise and support; and our amazing team of undergraduate researchers that helped us with all aspects of the animal work: Kimberly Straub, Brooke Salehzadeh, Abby Howell, Joette Crews, Aleia Hollands, Kathryn Sellman, Jessica Gladney, Caroline Coleman, Sarah Shaver, Shelley Tau, Jennifer Roveto, Madelaine Wendzik, Kayla Hargrove, Alexandra Ross, and Natalie Bishop. We would like to thank the following individuals for their assistance with MRI analysis and gait collection: Madelaine Wendzik and Elizabeth Waters. We would also like to thank Michael Larche and Samira Yeboah at the Center for Systems Imaging Core at Emory University for their MRI assistance.*

Author contributions: *Statistical analysis, data analysis and interpretation, manuscript writing: HW; design of study, collection and assembly of data, data analysis and interpretation: EWB; statistical analysis, data analysis and interpretation: AM; statistical analysis, data analysis and interpretation: RMP; conception and design of study, manuscript writing: FDW; conception and design of study, collection and assembly of data, data analysis and interpretation, manuscript writing: HAK.*

Conflicts of interest: *The authors have no conflicts of interest.*

Financial support: *Financial support was provided by the University of Georgia Office of the Vice President for Research to FDW.*

Data sharing statement: Datasets analyzed during the current study are available from the corresponding author on reasonable request.

Plagiarism check: *Checked twice by iThenticate.*

Peer review: *Externally peer reviewed.*

Additional file:

Additional Figure 1: *Experimental design.*

References

Allen KA (2016) Pathophysiology and treatment of severe traumatic brain injuries in children. J Neurosci Nurs 48:15-27; quiz E11.

Baker EW, Kinder HA, Hutcheson JM, Duberstein KJJ, Platt SR, Howerth EW, West FD (2019) Controlled cortical impact severity results in graded cellular, tissue, and functional responses in a piglet traumatic brain injury model. J Neurotrauma 36:61-73.

Beaumont A, Marmarou A, Czigner A, Yamamoto M, Demetriadou K, Shirotani T, Marmarou C, Dunbar J (1999) The impact-acceleration model of head injury: injury severity predicts motor and cognitive performance after trauma. Neurol Res 21:742-754.

Beretta E, Cimolin V, Piccinini L, Carla Turconi A, Galbiati S, Crivellini M, Galli M, Strazzer S (2009) Assessment of gait recovery in children after traumatic brain injury. Brain Inj 23:751-759.

Caeyenberghs K, Wenderoth N, Smits-Engelsman BC, Sunaert S, Swinnen SP (2009) Neural correlates of motor dysfunction in children with traumatic brain injury: exploration of compensatory recruitment patterns. Brain 132:684-694.

Caeyenberghs K, Leemans A, Geurts M, Taymans T, Linden CV, Smits-Engelsman BC, Sunaert S, Swinnen SP (2010) Brain-behavior relationships in young traumatic brain injury patients: DTI metrics are highly correlated with postural control. Hum Brain Mapp 31:992-1002.

Chastain CA, Oyoyo UE, Zipperman M, Joo E, Ashwal S, Shutter LA, Tong KA (2009) Predicting outcomes of traumatic brain injury by imaging modality and injury distribution. J Neurotrauma 26:1183-1196.

Chiewvit P, Tritakarn SO, Nanta-aree S, Suthipongchai S (2010) Degree of midline shift from CT scan predicted outcome in patients with head injuries. J Med Assoc Thai 93:99-107.

Chou LS, Kaufman KR, Walker-Rabatin AE, Brey RH, Basford JR (2004) Dynamic instability during obstacle crossing following traumatic brain injury. Gait Posture 20:245-254.

Conrad MS, Johnson RW (2015) The domestic piglet: an important model for investigating the neurodevelopmental consequences of early life insults. Annu Rev Anim Biosci 3:245-264.

Conrad MS, Dilger RN, Johnson RW (2012) Brain growth of the domestic pig (Sus scrofa) from 2 to 24 weeks of age: a longitudinal MRI study. Dev Neurosci 34:291-298.

Cooper JM, Catroppa C, Beauchamp MH, Eren S, Godfrey C, Ditchfield M, Anderson VA (2014) Attentional control ten years post-childhood traumatic brain injury: the impact of lesion presence, location, and severity in adolescence and early adulthood. J Neurotrauma 31:713-721.

Costine BA, Missios S, Taylor SR, McGuone D, Smith CM, Dodge CP, Harris BT, Duhaime AC (2015) The subventricular zone in the immature piglet brain: anatomy and exodus of neuroblasts into white matter after traumatic brain injury. Dev Neurosci 37:115-130.

Dobbing J, Sands J (1979) Comparative aspects of the brain growth spurt. Early Hum Dev 3:79-83.

Drijkoningen D, Chalavi S, Sunaert S, Duysens J, Swinnen SP, Caeyenberghs K (2017) Regional gray matter volume loss is associated with gait impairments in young brain-injured individuals. J Neurotrauma 34:1022-1034.

Duhaime AC, Hunter JV, Grate LL, Kim A, Golden J, Demidenko E, Harris C (2003) Magnetic resonance imaging studies of age-dependent responses to scaled focal brain injury in the piglet. J Neurosurg 99:542-548.

Englander J, Cifu DX, Wright JM, Black K (2003) The association of early computed tomography scan findings and ambulation, self-care, and supervision needs at rehabilitation discharge and at 1 year after traumatic brain injury. Arch Phys Med Rehabil 84:214-220.

Faul M, Xu L, Wald MM, Coronado VG (2010) Traumatic Brain Injury in the United States: Emergency Department Visits, Hospitalizations, and Deaths 2002–2006. Atlanta (GA): Centers for Disease Control and Prevention, National Center for Injury Prevention and Control.

Flynn TJ (1984) Developmental changes of myelin-related lipids in brain of miniature swine. Neurochem Res 9:935-945.

Gagnon I, Swaine B, Friedman D, Forget R (2004) Children show decreased dynamic balance after mild traumatic brain injury. Arch Phys Med Rehabil 85:444-452.

Galloway NR, Tong KA, Ashwal S, Oyoyo U, Obenaus A (2008) Diffusion-weighted imaging improves outcome prediction in pediatric traumatic brain injury. J Neurotrauma 25:1153-1162.

Gieling ET, Schuurman T, Nordquist RE, van der Staay FJ (2011) The pig as a model animal for studying cognition and neurobehavioral disorders. Curr Top Behav Neurosci 7:359-383.

Grate LL, Golden JA, Hoopes PJ, Hunter JV, Duhaime AC (2003) Traumatic brain injury in piglets of different ages: techniques for lesion analysis using histology and magnetic resonance imaging. J Neurosci Methods 123:201-206.

Guild EB, Levine B (2015) Functional correlates of midline brain volume loss in chronic traumatic brain injury. J Int Neuropsychol Soc 21:650-655.

Immonen RJ, Kharatishvili I, Grohn H, Pitkanen A, Grohn OH (2009) Quantitative MRI predicts long-term structural and functional outcome after experimental traumatic brain injury. Neuroimage 45:1-9.

Irimia A, Wang B, Aylward SR, Prastawa MW, Pace DF, Gerig G, Hovda DA, Kikinis R, Vespa PM, Van Horn JD (2012) Neuroimaging of structural pathology and connectomics in traumatic brain injury: Toward personalized outcome prediction. Neuroimage Clin 1:1-17.

Jacobs B, Beems T, van der Vliet TM, Diaz-Arrastia RR, Borm GF, Vos PE (2011) Computed tomography and outcome in moderate and severe traumatic brain injury: hematoma volume and midline shift revisited. J Neurotrauma 28:203-215.

Jaffe KM, Fay GC, Polissar NL, Martin KM, Shurtleff HA, Rivara JM, Winn HR (1993) Severity of pediatric traumatic brain injury and neurobehavioral recovery at one year--a cohort study. Arch Phys Med Rehabil 74:587-595.

Jain KK (2008) Neuroprotection in traumatic brain injury. Drug Discov Today 13:1082-1089.

Karlsson M, Pukenas B, Chawla S, Ehinger JK, Plyler R, Stolow M, Gabello M, Hugerth M, Elmer E, Hansson MJ, Margulies S, Kilbaugh T (2018) Neuroprotective effects of cyclosporine in a porcine pre-clinical trial of focal traumatic brain injury. J Neurotrauma doi: 10.1089/neu.2018.5706.

Katz-Leurer M, Rotem H, Keren O, Meyer S (2009a) The relationship between step variability, muscle strength and functional walking performance in children with post-traumatic brain injury. Gait Posture 29:154-157.

Katz-Leurer M, Rotem H, Keren O, Meyer S (2009b) Balance abilities and gait characteristics in post-traumatic brain injury, cerebral palsy and typically developed children. Dev Neurorehabil 12:100-105.

Kinder HA, Baker EW, West FD (2019a) The pig as a preclinical traumatic brain injury model: current models, functional outcome measures, and translational detection strategies. Neural Regen Res 14:413-424.

Kinder HA, Baker EW, Wang S, Fleischer CC, Howerth EW, Duberstein KJ, Mao H, Platt SR, West FD (2019b) Traumatic brain injury results in dynamic brain structure changes leading to acute and chronic motor function deficits in a pediatric piglet model. J Neurotrauma 36:2930-2942.

Kuhtz-Buschbeck JP, Hoppe B, Golge M, Dreesmann M, Damm-Stunitz U, Ritz A (2003) Sensorimotor recovery in children after traumatic brain injury: analyses of gait, gross motor, and fine motor skills. Dev Med Child Neurol 45:821-828.

Lee SY, Kim SS, Kim CH, Park SW, Park JH, Yeo M (2012) Prediction of outcome after traumatic brain injury using clinical and neuroimaging variables. J Clin Neurol 8:224-229.

Marklund N (2016) Rodent models of traumatic brain injury: methods and challenges. Methods Mol Biol 1462:29-46.

Martinez BI, Stabenfeldt SE (2019) Current trends in biomarker discovery and analysis tools for traumatic brain injury. J Biol Eng 13:16.

Martini DN, Sabin MJ, DePesa SA, Leal EW, Negrete TN, Sosnoff JJ, Broglio SP (2011) The chronic effects of concussion on gait. Arch Phys Med Rehabil 92:585-589.

Mateos-Perez JM, Dadar M, Lacalle-Aurioles M, Iturria-Medina Y, Zeighami Y, Evans AC (2018) Structural neuroimaging as clinical predictor: A review of machine learning applications. Neuroimage Clin 20:506-522.

Paredes MF, James D, Gil-Perotin S, Kim H, Cotter JA, Ng C, Sandoval K, Rowitch DH, Xu D, McQuillen PS, Garcia-Verdugo JM, Huang EJ, Alvarez-Buylla A (2016) Extensive migration of young neurons into the infant human frontal lobe. Science 354. pii: aaf7073.

Puffer RC, Yue JK, Mesley M, Billigen JB, Sharpless J, Fetzick AL, Puccio A, Diaz-Arrastia R, Okonkwo DO (2018) Long-term outcome in traumatic brain injury patients with midline shift: a secondary analysis of the Phase 3 COBRIT clinical trial. J Neurosurg 131:596-603.

R Core Team (2013) R: A language and environment for statistical computing. In: R Foundation for Statistical Computing. Vienna, Austria.

Rosenthal G, Morabito D, Cohen M, Roeytenberg A, Derugin N, Panter SS, Knudson MM, Manley G (2008) Use of hemoglobin-based oxygen-carrying solution-201 to improve resuscitation parameters and prevent secondary brain injury in a swine model of traumatic brain injury and hemorrhage: laboratory investigation. J Neurosurg 108:575-587.

Saatman KE, Duhaime AC, Bullock R, Maas AI, Valadka A, Manley GT; Workshop Scientific Team and Advisory Panel Members (2008) Classification of traumatic brain injury for targeted therapies. J Neurotrauma 25:719-738.

Sauvigny T, Gottsche J, Vettorazzi E, Westphal M, Regelsberger J (2016) New radiologic parameters predict clinical outcome after decompressive craniectomy. World Neurosurg 88:519-525.

Schindelin J, Rueden CT, Hiner MC, Eliceiri KW (2015) The ImageJ ecosystem: An open platform for biomedical image analysis. Mol Reprod Dev 82:518-529.

Sigmund GA, Tong KA, Nickerson JP, Wall CJ, Oyoyo U, Ashwal S (2007) Multimodality comparison of neuroimaging in pediatric traumatic brain injury. Pediatr Neurol 36:217-226.

Smitherman E, Hernandez A, Stavinoha PL, Huang R, Kernie SG, Diaz-Arrastia R, Miles DK (2016) Predicting outcome after pediatric traumatic brain injury by early magnetic resonance imaging lesion location and volume. J Neurotrauma 33:35-48.

Swanson JO, Vavilala MS, Wang J, Pruthi S, Fink J, Jaffe KM, Durbin D, Koepsell T, Temkin N, Rivara FP (2012) Association of initial CT findings with quality-of-life outcomes for traumatic brain injury in children. Pediatr Radiol 42:974-981.

Taylor CA, Bell JM, Breiding MJ, Xu L (2017) Traumatic brain injury-related emergency department visits, hospitalizations, and deaths- United States, 2007 and 2013. MMWR Surveill Summ 66:1-16.

Tsenter J, Beni-Adani L, Assaf Y, Alexandrovich AG, Trembovler V, Shohami E (2008) Dynamic changes in the recovery after traumatic brain injury in mice: effect of injury severity on T2-weighted MRI abnormalities, and motor and cognitive functions. J Neurotrauma 25:324-333.

Washington PM, Forcelli PA, Wilkins T, Zapple DN, Parsadanian M, Burns MP (2012) The effect of injury severity on behavior: a phenotypic study of cognitive and emotional deficits after mild, moderate, and severe controlled cortical impact injury in mice. J Neurotrauma 29:2283-2296.

Williams G, Morris ME, Schache A, McCrory PR (2009) Incidence of gait abnormalities after traumatic brain injury. Arch Phys Med Rehabil 90:587-593.

Williams G, Galna B, Morris ME, Olver J (2010) Spatiotemporal deficits and kinematic classification of gait following a traumatic brain injury: a systematic review. J Head Trauma Rehabil 25:366-374.

Ziebell JM, Morganti-Kossmann MC (2010) Involvement of pro- and anti-inflammatory cytokines and chemokines in the pathophysiology of traumatic brain injury. Neurotherapeutics 7:22-30.

C-Editors: Zhao M, Li CH; T-Editor: Jia Y